Advanced Glycation End Products in Extracellular Matrix Proteins Contribute to the Failure of Sensory Nerve Regeneration in Diabetes

Beatriz Duran-Jimenez,[1] Darin Dobler,[2] Sarah Moffatt,[1] Naila Rabbani,[2] Charles H. Streuli,[1] Paul J. Thornalley,[2] David R. Tomlinson,[1] and Natalie J. Gardiner[1]

OBJECTIVE—The goal of this study was to characterize glycation adducts formed in both in vivo extracellular matrix (ECM) proteins of endoneurium from streptozotocin (STZ)-induced diabetic rats and in vitro by glycation of laminin and fibronectin with methylglyoxal and glucose. We also investigated the impact of advanced glycation end product (AGE) residue content of ECM on neurite outgrowth from sensory neurons.

RESEARCH DESIGN AND METHODS—Glycation, oxidation, and nitration adducts of ECM proteins extracted from the endoneurium of control and STZ-induced diabetic rat sciatic nerve (3–24 weeks post-STZ) and of laminin and fibronectin that had been glycated using glucose or methylglyoxal were examined by liquid chromatography with tandem mass spectrometry. Methylglyoxal-glycated or unmodified ECM proteins were used as substrata for dissociated rat sensory neurons as in vitro models of regeneration.

RESULTS—STZ-induced diabetes produced a significant increase in early glycation N_ε-fructosyl-lysine and AGE residue contents of endoneurial ECM. Glycation of laminin and fibronectin by methylglyoxal and glucose increased glycation adduct residue contents with methylglyoxal-derived hydroimidazolone and N_ε-fructosyl-lysine, respectively, of greatest quantitative importance. Glycation of laminin caused a significant decrease in both neurotrophin-stimulated and preconditioned sensory neurite outgrowth. This decrease was prevented by aminoguanidine. Glycation of fibronectin also decreased preconditioned neurite outgrowth, which was prevented by aminoguanidine and nerve growth factor.

CONCLUSIONS—Early glycation and AGE residue content of endoneurial ECM proteins increase markedly in STZ-induced diabetes. Glycation of laminin and fibronectin causes a reduction in neurotrophin-stimulated neurite outgrowth and preconditioned neurite outgrowth. This may provide a mechanism for the failure of collateral sprouting and axonal regeneration in diabetic neuropathy. *Diabetes* **58:**2893–2903, 2009

The extracellular matrix (ECM) provides physical support for cells and tissue and also has a crucial role in regulating cell behavior and mediating survival, proliferation, differentiation, and migration via interaction with specific cell adhesion receptors such as integrins (1). Sensory neurons contain at least five laminin-binding integrins and two fibronectin-binding integrins (2–5), and we and others (3,6) have shown the β1-integrins to be crucial mediators of neuronal adhesion and nerve regeneration. Therefore, modification of ECM proteins by glycation in diabetes may have a severe impact on cellular function.

Glycation of proteins involves the covalent linkage of saccharides and saccharide derivatives to proteins. Glucose reacts with amino groups of lysine and NH_2-terminal amino acid residues. Early stage reactions lead to the formation of fructosyl-lysine and related fructosamine residues, which degrade slowly to form advanced glycation end products (AGEs). In addition to degradation of glycated proteins, glycolytic intermediates and lipid peroxidation lead to the formation of the reactive dicarbonyl metabolites, glyoxal, methylglyoxal, and 3-deoxyglucosone (3-DG). Dicarbonyls form AGE residues in proteins largely, but not exclusively, on arginine residues. At the quantitative level, the most abundant AGEs are the hydroimidazolones derived from glyoxal, methylglyoxal, and 3-DG (denoted by the acronyms G-H1, MG-H1, and 3DG-H), the lysine-derived AGEs (N_ε-carboxymethyl-lysine [CML] and N_ε-carboxyethyllysine [CEL]), imidazolium cross-links derived from glyoxal, methylglyoxal, and 3-DG (GOLD, MOLD, and DOLD), and the trace fluorescent cross-link pentosidine.

AGE residues accumulate in both intracellular and extracellular proteins, especially in those with poorly controlled diabetes and tissues with metabolic dysfunction associated with high cellular glucose concentration. Accumulation of AGE residues is a risk marker for the development of diabetic neuropathy (7–9). AGE formation can be decreased by scavenging dicarbonyl precursors with aminoguanidine (10), which suppresses neurovascular dysfunction in streptozotocin (STZ)-induced diabetic rats (11,12).

ECM proteins are particularly long-lived, and they are potential targets of glycation. Changes in the composition and structure of ECM of peripheral nerve are observed in those with diabetes; notably increased endoneurial collagen, reduplication of basement membranes around endoneurial capillaries, and a thickening of basal lamina are present in both clinical and experi-

mental diabetes (13–16). Glycation of ECM proteins modifies functionally important arginine residues of RGD (arg-gly-asp) and GFOGER (gly-phe-hyp-gly-glu-arg) motifs causing loss of charge and structural distortion, which is associated with decreased binding affinity of integrins and cell detachment. It also produces intramolecular cross-linking, causing structural distortion, and may confer resistance to proteolysis, leading to thickening of the basement membrane (17).

We have previously shown that cytosolic protein extracts of peripheral nerve of STZ-induced diabetic rats have increased fructosyl-lysine and AGE residue content compared with controls (7). In this current study, we first characterized and quantified AGE residue content in ECM protein extracts from the endoneurium of STZ-induced diabetic rat sciatic nerve over a 24-week time point. Second, we glycated the ECM proteins, laminin and fibronectin, in vitro using glucose and methylglyoxal and characterized and quantified the AGE residue contents of these glycated and unmodified control proteins. To address the functional impact of increased AGE residue content in ECM proteins on axonal outgrowth, we used two in vitro models of sensory nerve regeneration to model both collateral sprouting and axonal regeneration processes.

RESEARCH DESIGN AND METHODS

Reagents. All chemicals were obtained from Sigma-Aldrich (Poole, Dorset, U.K.) unless otherwise stated. High-purity methylglyoxal was prepared by acid hydrolysis of freshly distilled methylglyoxal dimethylacetal and purified by fractional distillation under reduced pressure (18).

All studies and procedures were licensed under the U.K. Animals (Scientific Procedures) Act 1986. Diabetes was induced in adult female Wistar rats (200–250 g, Charles River, U.K.) via intraperitoneal injection of freshly dissolved STZ (55 mg/kg in sterile saline) as previously described (19). Rats were killed at various time points after induction of diabetes (3, 6, 9, 12, and 24 weeks post-STZ, $n = 6$ at each time point), and the sciatic nerves were rapidly removed and frozen on liquid nitrogen. Age- and weight-matched rats were used as nondiabetic controls (time 0 and 24 weeks, $n = 4$ at each time point).

A separate group of adult male Wistar rats (250–300 g, $n = 12$) were anesthetized with isofluorane (2% in oxygen) under sterile conditions, and the left sciatic nerve was exposed at mid-thigh level. The sciatic nerve was crushed with the tips of watchmakers forceps (2×15 s), the wound was closed, and animals recovered under observation. Seven days after nerve crush, rats were killed by concussion followed by decapitation. Ipsilateral and contralateral L4 and L5 dorsal root ganglia (DRG) were removed for cell culture experiments.

ECM protein extraction from sciatic endoneurium. Sciatic nerves were desheathed, homogenized in 0.25 mol/l sucrose on ice, and centrifuged at 900 g at 4°C. The ECM protein in the pellet was washed with PBS, then extracted with chloroform:methanol (2:1, v:v) and stirred continuously for 24 h at 4°C and centrifuged at 900 g at 4°C. The pellet was washed twice with PBS and frozen at −80°C until analysis.

Glycation of ECM proteins. Laminin and fibronectin modified by fructosyl-lysine and AGEs (AGE-laminin and AGE-fibronectin, respectively) were prepared by incubating the proteins (6.6 mg/ml) with 50 mmol/l glucose in 100 mmol/l sodium phosphate buffer, pH 7.4, at 37°C for 21 days. Laminin and fibronectin were also modified by incubating the proteins (6.6 mg/ml) with 500 µmol/l methylglyoxal in 100 mmol/l sodium phosphate buffer, pH 7.4, at 37°C for 24 h. After the incubation, glycated and control proteins were dialyzed against 30 mmol/l ammonium formate, pH 7.8 and 4°C; lyophilized to dryness; and stored at −20°C.

Protein glycation, oxidation, and nitration adduct determination by liquid chromatography–mass spectrometry/mass spectrometry. Protein glycation, oxidation, and nitration adducts were determined by stable isotopic dilution analysis liquid chromatography with tandem mass spectrophotometer detection (7). Glycation adducts determined were fructosyl-lysine and 10 AGEs (CML, CEL, G-H1, MG-H1, 3DG-H, GOLD, MOLD, DOLD, argpyrimidine, and pentosidine). The protein oxidation adduct dityrosine, the protein nitration adduct neurotrophin-3 (3-NT), and amino acids lys, arg, met, tyr, and trp were also determined. Pentosidine was determined by liquid chromatography

with fluorimetric detection (20). Authentic standard analyses were prepared as described (7,21). Glycation, oxidation, and nitration adduct residues of protein extracts were determined in exhaustive enzymatic digests (50 µg protein equivalent) (22). Samples were analyzed using a module 2690 separation module with a Quattro Ultima triple-quadrupole mass spectrometric detector and 2475 fluorescence detector (Waters-Micromass, Manchester, U.K.) as previously described (20).

Sensory neuron culture. Control or preconditioned (7 days postunilateral sciatic nerve crush injury) adult rat sensory neurons were mechanically and chemically dissociated, purified, and resuspended in modified Bottenstein and Sato's medium in Ham's F12 (containing 10 mmol/l D-glucose) as previously described (6,19,23).

Coating of slides with ECM. Labtek slides (VWR, U.K.) were either coated directly with 2 µg/ml laminin or derivatized for 30 min with 1 mmol/l m-maleimidobenzoyl-N-hydroxysuccinimide ester (Pierce Chemical, Rockford, IL) before coating for 1 h at room temperature with 10 µg/ml fibronectin (24). Methylglyoxal (500 µmol/l), aminoguanidine (500 µmol/l), methylglyoxal with aminoguanidine (both 500 µmol/l), or PBS was added to appropriate wells and slides incubated for 24 h at 37°C. Slides were washed three times and neurons were seeded onto slides in Bottenstein and Sato's medium and allowed to adhere to the substrate for 1 h before addition of nerve growth factor (NGF) (10 ng/ml) or glial cell-derived neurotrophic factor (GDNF) (50 ng/ml, Promega). Neurons were incubated for 18 h in 5% CO_2 at 37°C and immunostained with anti–β(III)-tubulin antibody (1:1,000, Sigma), a pan-neuronal marker labeling all cell bodies and neurites as previously described (23).

Neurite outgrowth analysis. For each experimental condition, images of neurons were acquired from 20 randomly selected fields of view per condition. Assessors were blinded to the experimental condition during analysis. The mean number of neurite-bearing cells was calculated (defined as those with neurites longer than 1.5 times the associated cell body diameter). The length of the longest neurite from each cell was calculated using SigmaScan software (SPSS, U.K.), as was a measure of total neurite outgrowth: a series of concentric circles was overlaid onto an image of each neuron, and the number of times neurites crossed each circle was calculated. This provided both a measure of total neurite outgrowth (total number of cross points) and neurite branching structure (cross points related to distance from the cell body). All these measurements were made from cells in the 20 randomly selected fields in each experiment and repeated in at least four independent cultures (23). Data are expressed as means ± SD. Statistical analysis was conducted using Graphpad Prizm software using ANOVA followed by Bonferroni post hoc test.

RESULTS

Glycation, oxidation, and nitration adduct residue content of endoneurial ECM proteins in experimental diabetes. To determine whether diabetes altered the extent of adduct residue content on endoneurial ECM proteins, we assessed 14 markers of glycation, oxidation, and nitration by liquid chromatography–mass spectrometry/mass spectrometry. Ten of the 14 markers investigated were present in detectable amounts in endoneurial ECM proteins from control and STZ-induced diabetic rats. These were fructosyl-lysine, CML, CEL, G-H1, MG-H1, 3DG-H, MOLD, pentosidine, MetSO, and dityrosine. The protein damage marker residues below the limit of detection (LOD) were GOLD, DOLD, argpyrimidine, and 3-NT. Estimates of pentosidine residues were <LOD in 33% of cases (STZ-induced diabetic study groups) and were set to the LOD in such cases for statistical analysis. For indexes of diabetes refer to Table 1.

After induction of diabetes, there were significant increases in the amount of fructosyl-lysine, CML, G-H1, and MG-H1 adduct residue contents on endoneurial ECM proteins (Fig. 1A–D). There were no significant changes in CEL (0.083 ± 0.025 mmol/mol lys), pentosidine (0.0016 ± 0.0009 mmol/mol lys), MOLD (0.004 ± 0.003 mmol/mol lys), MetSO (31.3 ± 8.7 mmol/mol met), and dityrosine (0.29 ± 0.13 mmol/mol tyr) residue contents and a onefold increase of 3DG-H residues (1.26 ± 0.69 vs. 0.67 ± 0.13 mmol/mol arg; $P < 0.05$) after 6 weeks of diabetes. For

TABLE 1
Indexes of STZ-induced diabetes over 24-week time period

Experimental group (n)	Body wt (g)		Terminal blood glucose levels (mmol/l)	Motor nerve conduction velocity (m/s)	Sensory nerve conduction velocity (m/s)
	Start	End			
Control 0	231 ± 10	231 ± 10	n.t.	n.t.	n.t.
Control 24 weeks	239 ± 5	361 ± 53	n.t.	58.7 ± 9.2	57 ± 4.8
STZ 3 weeks	233 ± 7	215 ± 21	26 ± 3.7	n.t.	n.t.
STZ 6 weeks	242 ± 10	257 ± 15	26.9 ± 1.4	n.t.	n.t.
STZ 9 weeks	242 ± 17	271 ± 27	25.4 ± 2.9	n.t.	n.t.
STZ 12 weeks	233 ± 13	264 ± 41	21.5 ± 7.6	n.t.	n.t.
STZ 24 weeks	233 ± 16	319 ± 55	23.3 ± 7.9	43.2 ± 5.4*	45.5 ± 3.9*

Data are means ± SD unless otherwise indicated. *$P < 0.005$: t test, control vs. diabetic nerve conduction velocity at 24 weeks. n.t. = not tested.

MG-H1, there was a relative decline at weeks 9 and 12 of diabetes after reaching a maximum content at 6 weeks of diabetes and rebound to higher contents after 24 weeks. There were no age-related changes in adduct residue contents over the 24-week time course studied (Fig. 1A–D; no significant differences in AGE content between endoneurial ECM protein samples at time 0 or 24 weeks post-STZ; $P > 0.05$). These results indicate that the increase in fructosyl-lysine, CML, G-H1, and MG-H1 residue contents of ECM proteins of the sciatic nerve endoneurium correlates with the development of STZ-induced diabetes.

Glycation of ECM proteins by methylglyoxal and glucose in vitro. To test the hypothesis that ECM proteins are susceptible to glycation under physiological conditions, we incubated laminin and fibronectin with methylglyoxal or glucose. Note that similar conditions

used with human serum albumin (HSA) produced HSA modified minimally with glycation adducts (1–2 molar equivalents) (25). Control fibronectin and laminin had minor but significant contents of glycation adducts fructosyl-lysine, CML, MG-H1, and 3DG-H, ranging from 0.2–2.3 mol/mol protein and some protein oxidation (1–6 equivalents of MetSO residues) but no detectable dityrosine or 3-NT (Tables 2 and 3).

Glycation of fibronectin by methylglyoxal produced ~28 equivalents of MG-H1. This was the major methylglyoxal-derived AGE formed (97%), the others being CEL (0.06 mol; 0.2%), argpyrimidine (0.79 mol; 3%), and MOLD (0.002 mol; 0.01%); the total methylglyoxal-derived adduct increase was ~29.2 molar equivalents, representing 88% of the added methylglyoxal (Table 2). Similarly, glycation of laminin by methylglyoxal produced ~56 equivalents of MG-H1 (88%), together with CEL (0.53 mol: 0.8%), argpyri-
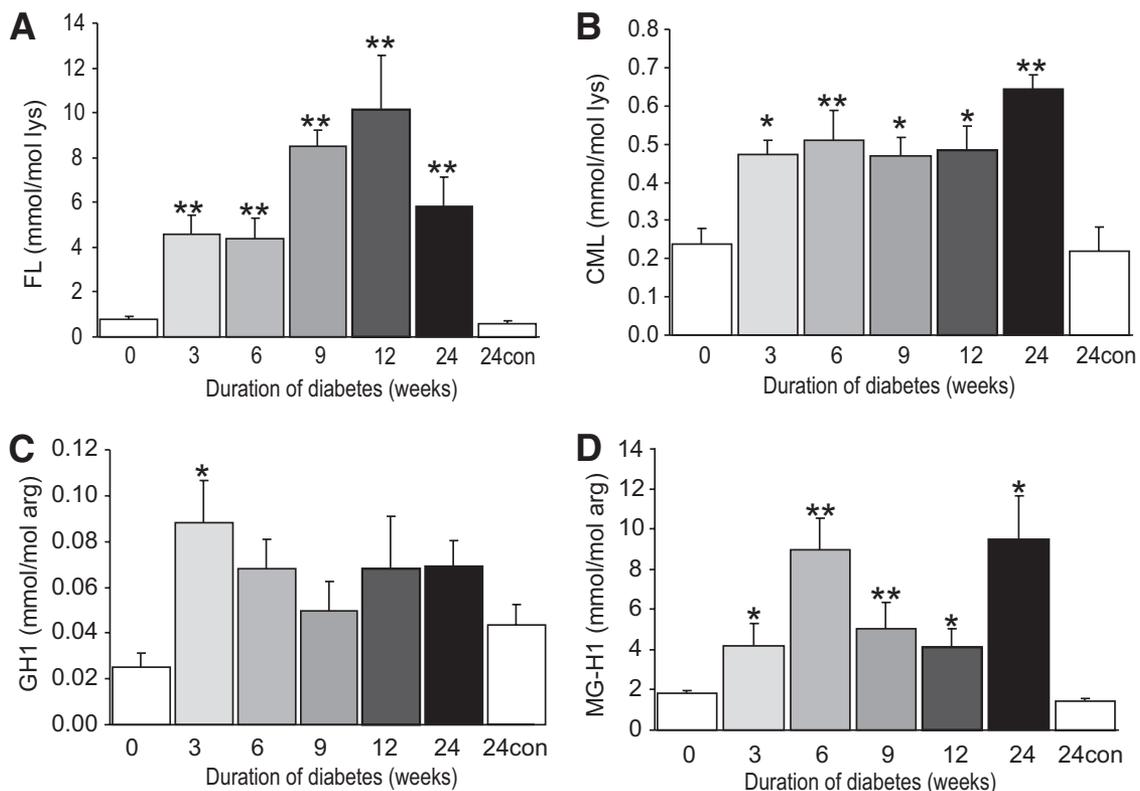
FIG. 1. Glycation adduct content of endoneurial ECM proteins of STZ-induced diabetic rat sciatic nerve. N_ε-fructosyl-lysine (A), CML (B), G-H1 (C), and MG-H1 (D). Data are given for nondiabetic control (con) rats at 0 and 24 weeks of the experiment and for STZ-induced diabetic rats with duration of diabetes 3–24 weeks (post–STZ injection). Data are means ± SE ($n = 6$–8 for STZ-induced diabetic groups; $n = 4$ for nondiabetic controls). Significance: *$P < 0.05$, **$P < 0.01$ compared with nondiabetic controls (Kruskal-Wallis). FL, fructosyl-lysine.

TABLE 2
Glycation adduct residue contents of human fibronectin glycated by methylglyoxal and glucose (AGE)

Glycation adduct	Methylglyoxal-fibronectin control-1*	Methylglyoxal-fibronectin	AGE-fibronectin control-2†	AGE-fibronectin
Fructosyl-lysine	0.213 ± 0.034	0.215 ± 0.088	0.094 ± 0.022	$0.610 \pm 0.088¶$
CML	0.119 ± 0.025	$0.202 \pm 0.041‡$	0.079 ± 0.021	0.092 ± 0.020
CEL	0.008 ± 0.001	$0.067 \pm 0.016‡$	0.007 ± 0.001	0.014 ± 0.005
G-H1	0.016 ± 0.004	$0.046 \pm 0.007§$	0.005 ± 0.002	0.008 ± 0.001
MG-H1	0.239 ± 0.013	$28.42 \pm 0.97¶$	0.176 ± 0.006	$0.198 \pm 0.006‡$
3DG-H	0.217 ± 0.068	0.819 ± 0.215	0.420 ± 0.066	$0.727 \pm 0.044§$
Argpyrimidine	<LOD	$0.793 \pm 0.060¶$	<LOD	<LOD
MOLD	0.0021 ± 0.0001	$0.0039 \pm 0.0003¶$	0.0015 ± 0.0001	0.0030 ± 0.0008
Pentosidine	0.000015 ± 0.000001	$0.000129 \pm 0.000010¶$	0.000007 ± 0.000001	$0.000012 \pm 0.000001¶$
MetSO	1.05 ± 0.09	$3.15 \pm 0.16¶$	0.40 ± 0.04	0.38 ± 0.02

Data are mol/mol fibronectin; means $\pm$ SD ($n = 3$). *Fibronectin incubated under the conditions to control for glycation by methylglyoxal. †Fibronectin incubated under the conditions to control for glycation by glucose. <LOD indicates argpyrimidine residue content is less than the limit of detection (<0.001 mol/mol fibronectin). Other adducts not detected were (mol/mol): GOLD and dityrosine <0.0006, DOLD <0.0002, and 3-NT <0.0001. ‡$P < 0.05$, §$P < 0.01$, ¶$P < 0.001$; t test.

midine (6.8 mol; 11%), and MOLD (0.04 mol; 0.07%). The total adduct methylglyoxal-derived adduct increase was ~63.1 molar equivalents, representing 93% of the added methylglyoxal (Table 3).

Glycation of fibronectin by glucose gave a relatively modest increase in glycation adduct residues: fructosyl-lysine (0.52 mol; 61% detected adduct residue increase), 3DG-H (0.32 mol; 36%), and trace amounts of MG-H1 and pentosidine (Table 2). Glycation of laminin by glucose gave much higher increases of glycation adduct residues: fructosyl-lysine (21 mol; 81%), 3DG-H (3.7 mol; 14%), CML (1.1 mol; 4%), G-H1 (0.2 mol; 0.8%), and trace amounts of CEL, MOLD, and pentosidine. As expected, pentosidine residue content was very low in all proteins analyzed, <0.01 mol% (Table 3).

Sensory nerve regeneration is impaired on glycated ECM. Because experiments using function-blocking antibodies have highlighted the essential role that laminin and fibronectin play in promoting axonal outgrowth, we hypothesized that glycation of these proteins may contribute directly to failure of axonal regeneration (26,27).

To test this hypothesis, we examined the ability of dissociated adult rat sensory neurons to form neurites in culture. The addition of neurotrophic factors during the first 18 h promotes neurite outgrowth in defined populations of sensory neurons, which enabled us to compare regeneration of different populations of neurons on glycated versus unmodified laminin and fibronectin. Sensory neurons in culture exhibit two distinct forms of neurite outgrowth: an initial, short arborizing form of neurite outgrowth, which occurs in the absence of neurotrophic factors (but is enhanced by addition of NGF, NT-3, or GDNF), followed by a transcription-dependent switch to axon elongation. The arborizing growth is analogous to the collateral sprouting of terminal fields seen in vivo, whereas elongation is analogous to axon regeneration in vivo (28).

Survival of sensory neurons was not altered on methylglyoxal-glycated laminin in comparison to untreated laminin (assessed using trypan blue 18 h after plating, data not shown), nor was the percentage of neurite-bearing cells (Fig. 2D).

Neurons plated on laminin extended highly arborised neurites in the presence of NGF (Fig. 2A). In contrast, neurite outgrowth was dramatically lower on methylglyoxal-glycated laminin (Fig. 2B). Quantification of NGF-stimulated neurite outgrowth showed no significant decrease in the length of longest neurite (Fig. 2E) but significant reduction in total neurite density and branching, as measured by cross-point analysis (total neurite density: laminin 160 $\pm$ 28 cross points vs. methylglyoxal-glycated laminin 90 $\pm$ 18 cross points, $P <$ 0.05; at 100 μm from cell body: laminin 32 $\pm$ 3 cross points vs. methylglyoxal-glycated laminin 17.4 $\pm$ 3 cross points, $P <$

TABLE 3
Glycation adduct contents of laminin minimally modified by methylglyoxal and glucose (AGE)

Glycation adduct	Methylglyoxal-laminin control-1*	Methylglyoxal-laminin	AGE-laminin control-2†	AGE-laminin
FL	0.777 ± 0.100	0.698 ± 0.047	1.11 ± 0.35	$21.84 \pm 0.58¶$
CML	0.303 ± 0.052	0.332 ± 0.070	0.353 ± 0.027	$1.420 \pm 0.094¶$
CEL	0.035 ± 0.009	$0.562 \pm 0.047¶$	0.029 ± 0.004	$0.055 \pm 0.010‡$
G-H1	0.022 ± 0.009	0.021 ± 0.011	0.031 ± 0.001	$0.229 \pm 0.060§$
MG-H1	0.87 ± 0.04	$56.57 \pm 1.78¶$	1.44 ± 0.10	1.66 ± 0.16
3DG-H	2.31 ± 0.29	$1.34 \pm 0.36‡$	2.26 ± 0.16	$5.97 \pm 0.57§$
Argpyrimidine	<LOD	6.82 ± 0.56	<LOD	<LOD
MOLD	0.0030 ± 0.0011	$0.0448 \pm 0.0081‡$	0.0018 ± 0.0006	$0.0074 \pm 0.0012§$
Pentosidine	0.000036 ± 0.000002	$0.000045 \pm 0.000001‡$	0.000052 ± 0.000002	$0.000089 \pm 0.000004¶$
MetSO	6.01 ± 0.23	5.91 ± 1.56	4.81 ± 0.88	3.89 ± 1.32

Data are mol/mol laminin; means $\pm$ SD ($n = 3$). <LOD indicates argpyrimidine residue content is less than the limit of detection (<0.002 mol/mol laminin). Other adducts not detected were (mol/mol): GOLD and dityrosine <0.0012, DOLD <0.0004, and 3-NT <0.0002. *Laminin incubated under the conditions to control for glycation by methylglyoxal. †Laminin incubated under the conditions to control for glycation by glucose. ‡$P < 0.05$, §$P < 0.01$, ¶$P < 0.001$; t test.
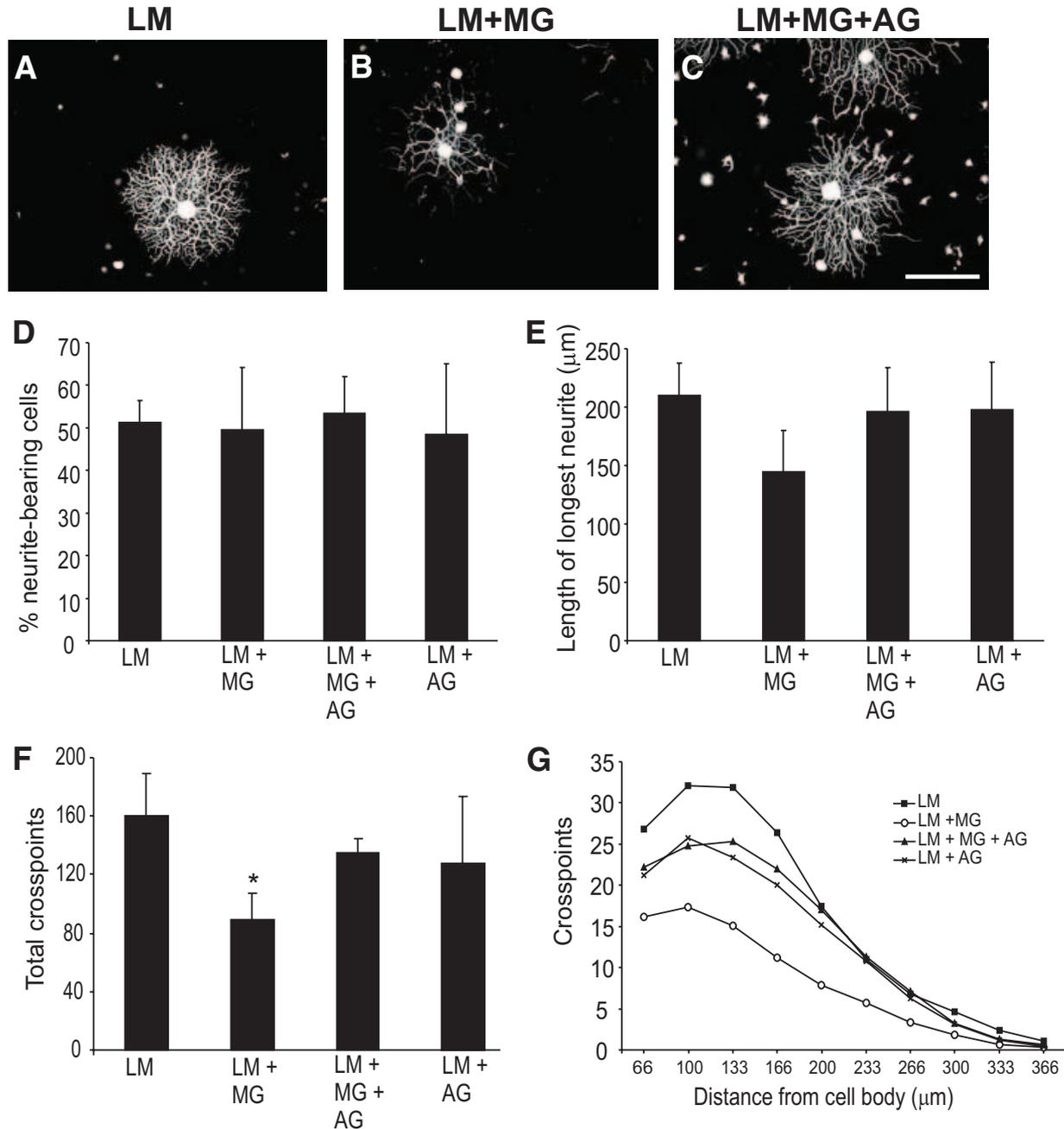
FIG. 2. Sensory neurons plated on glycated laminin and treated with NGF extend fewer, less-branched neurites than those plated on control unmodified laminin. Representative photomicrographs of sensory neurons plated on laminin (*A*), laminin glycated with methylglyoxal (*B*), or laminin treated with methylglyoxal in the presence of aminoguanidine (*C*). NGF treatment (10 ng/ml; 18 h) stimulated neurons plated on laminin to extend elaborate highly branched neurites (*A*). In contrast, NGF-stimulated neurite outgrowth on methylglyoxal-glycated laminin was much less extensive (*B*); this was prevented by inclusion of aminoguanidine (*C*). Quantification of NGF-stimulated neurite outgrowth showed no significant reduction in length of longest neurite (*E*) but a significant reduction in total neurite density and branching structure, compared with control, as measured by cross-point analysis (*F* and *G*), which was prevented by inclusion of the glycation scavenger aminoguanidine (*C*, *F*, and *G*). Data are expressed as means ± SD; *n* = 4 independent cultures (ANOVA and Bonferroni multiple-comparison post hoc test, *$P < 0.05$). Aminoguanidine treatment alone had no significant effect on any of the indexes examined (*D–G*; $P > 0.05$). Scale bar = 100 μm. AG, aminoguanidine; LM, laminin; MG, methylglyoxal.

0.001; Fig. 2*F* and *G*). Typically, the neurons that extended neurites in response to NGF on glycated laminin had fewer and less-branched neurites than those plated on control unmodified laminin. To confirm this decrease was associated with glycation, methylglyoxal-glycation was conducted in the presence of the glycation scavenger aminoguanidine, which prevented the deficits in neurite outgrowth (Fig. 2*C*, *F*, and *G*).

The GDNF-responsive subpopulation of neurons was similarly disadvantaged when plated on glycated laminin

(Fig. 3). There were significant glycation-associated decreases in the length of longest neurite (Fig. 3*B* and *E*), total neurite outgrowth (total neurite density: 64.7 ± 28.6 cross points on laminin vs. 21.2 ± 18.2 cross points on methylglyoxal-glycated laminin, $P < 0.05$; Fig. 3*B* and *F*) and a reduction in branching structure (Fig. 3*B* and *G*). These deficits were also prevented by inclusion of aminoguanidine.

Diabetes is associated with the initial presence of regenerative axon profiles alongside degenerative struc-
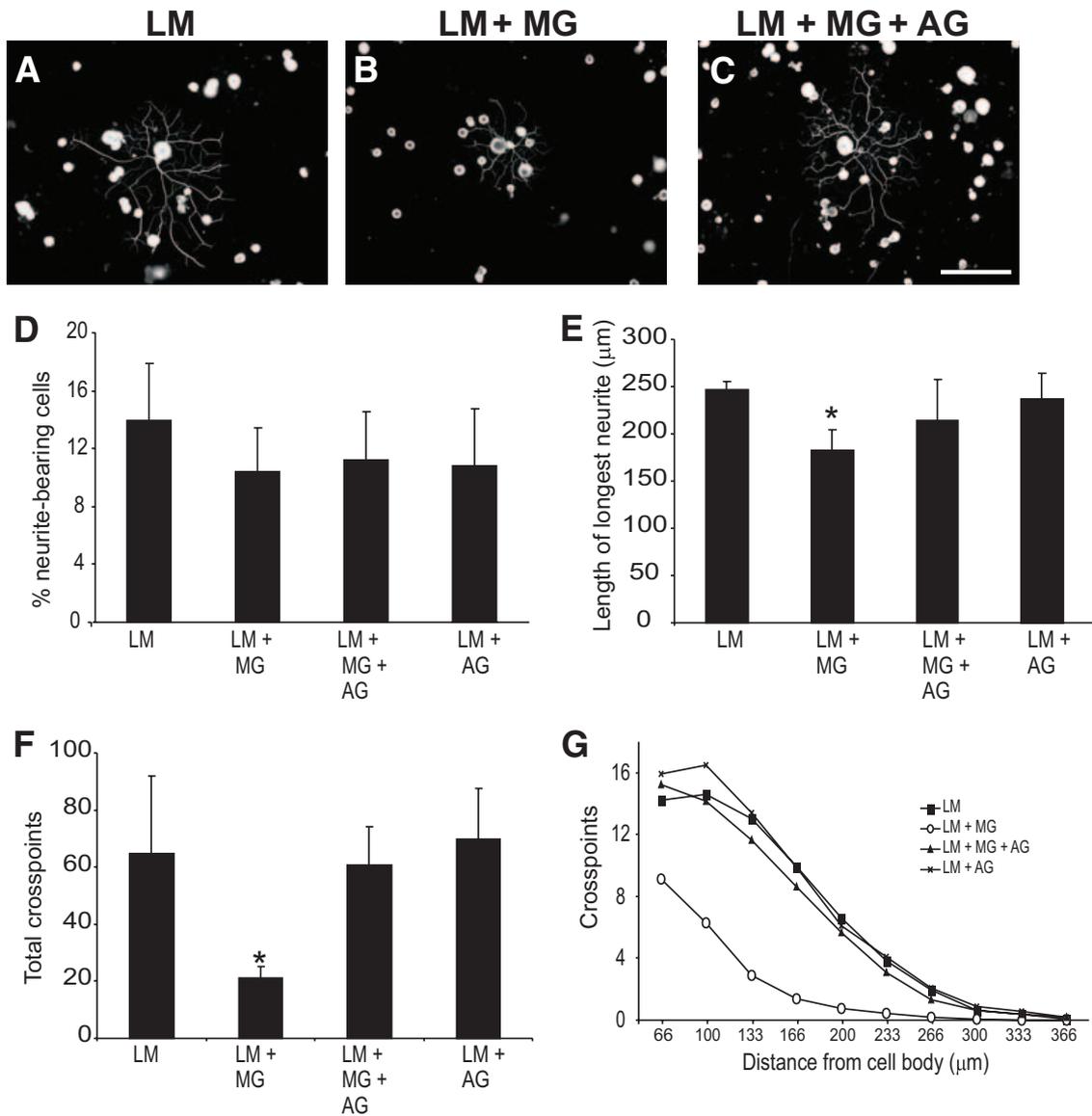
FIG. 3. GDNF-induced neurite outgrowth is reduced from sensory neurons plated on glycated laminin. Representative photomicrographs of sensory neurons plated on laminin (*A*), laminin glycated with methylglyoxal (*B*), or laminin treated with methylglyoxal in the presence of aminoguanidine (*C*). GDNF treatment (50 ng/ml; 18 h) stimulated neurons plated on laminin to extend elaborate highly branched neurites (*A*). In contrast, GDNF-stimulated neurite outgrowth on methylglyoxal-glycated laminin was much less extensive (*B*); this was prevented by inclusion of aminoguanidine (*C*). Quantification of GDNF-stimulated neurite outgrowth showed a significant reduction in length of longest neurite (*D*), total neurite density, and branching structure compared with control, as measured by cross-point analysis (*F* and *G*), which was prevented by inclusion of the glycation scavenger aminoguanidine (*C*, *F*, and *G*). Data are expressed as means ± SD, $n = 4$ independent cultures (ANOVA and Bonferroni multiple-comparison post hoc test, *$P < 0.05$). Aminoguanidine treatment alone had no significant effect on any of the indexes examined (*D–G*; $P > 0.05$). Scale bar = 100 μm. AG, aminoguanidine; LM, laminin; MG, methylglyoxal.

tures in peripheral nerve (29). To model this regenerative phenotype, we used a preconditioning nerve-crush injury model that can potentiate the capacity of sensory neurons to mount a regenerative response after a subsequent injury to their axons (30,31). Control sensory neurons extend neurites very poorly on fibronectin compared with growth on laminin; however, neurite outgrowth is enhanced by a preconditioning crush to the sciatic nerve in vivo 7 days before culture (23). Therefore, we used this model to investigate the impact of glycation of laminin and fibronectin on sensory nerve regeneration.

Preconditioned neurons plated on laminin extended some neurites even in the absence of exogenous neurotrophins (Fig. 4*A*), but growth was strongly enhanced by addition of NGF (Fig. 4*D*) or GDNF (Fig. 4*G*). Glycation of

laminin significantly reduced preconditioned neurite outgrowth in all treatment conditions (Fig. 4*B*, *E*, and *H*). This reduction was prevented by inclusion of aminoguanidine (Fig. 4*C*, *F*, and *I*). Quantification of preconditioned neurite outgrowth showed significant glycation-associated decreases in the length of longest neurite and total neurite density (Fig. 4*J* and *K*).

Preconditioned neurite outgrowth was also observed on fibronectin in the absence of neurotrophic support (Fig. 5*A*), which was strongly enhanced by GDNF but not NGF (in agreement with our previous study [23]). In neurons plated on glycated fibronectin, neurite outgrowth was significantly impaired, both in the absence of neurotrophins and in the presence of GDNF (Fig. 5*B*, *D*, *J*, and *K*). As before, inclusion of aminoguanidine prevented the glycation-mediated inhibition. Interestingly, the addition of NGF to preconditioned
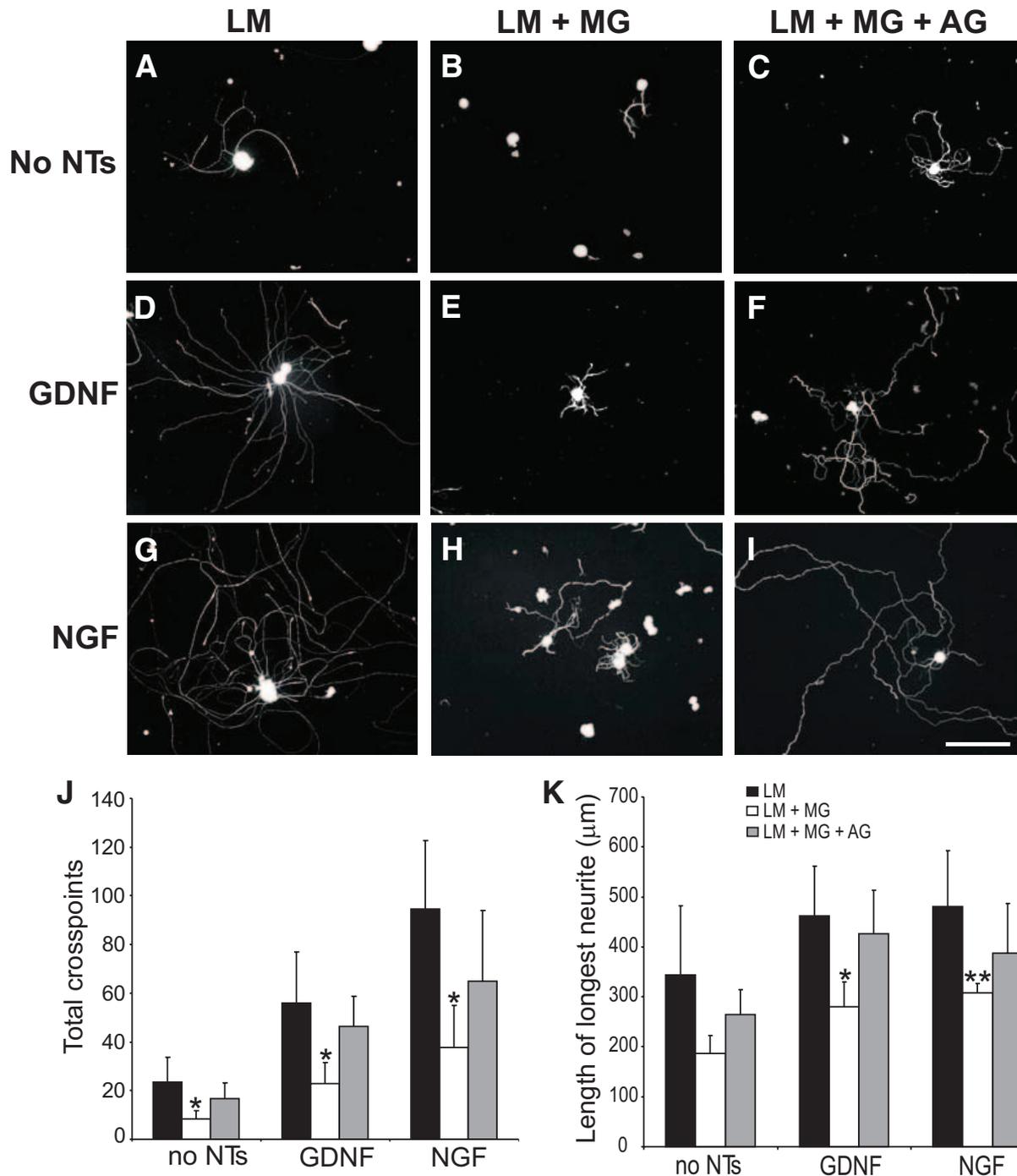
FIG. 4. Enhanced neurite outgrowth in response to a preconditioning sciatic nerve crush is reduced in neurons plated on glycated laminin. Representative photomicrographs of neurons from L4 and L5 DRG ipsilateral to a crush injury to the sciatic nerve (7 days before culture), which were dissociated and plated on laminin (A, D, and G), laminin glycated with methylglyoxal (B, E, and H), or laminin treated with methylglyoxal in the presence of aminoguanidine (C, F, and I) for 18 h with (D–I) or without (A–C) neurotrophin treatment (D–F, 50 ng/ml GDNF; G–I, 10 ng/ml NGF). The preconditioned neurons extend neurites in the absence of neurotrophic support (A–C); this was enhanced by neurotrophin treatment (D–I). Two parameters of neurite extension were quantified: total neurite outgrowth (J, cross points) and length of longest neurite (K). Neurons plated on glycated laminin showed a significant reduction in length of longest neurite and total neurite density compared with control, which was prevented by inclusion of the glycation scavenger aminoguanidine (C, F, and I–K). All data are expressed as means ± SD, $n = 4$ independent experiments (ANOVA with Bonferroni post hoc test, $*P < 0.05$, $**P < 0.01$). Scale bar = 100 μm. AG, aminoguanidine; LM, laminin; MG, methylglyoxal.

neurons also prevented glycation-mediated inhibition of neurite outgrowth (Fig. 5J and K).

These results show that ECM glycation has a dramatic inhibitory effect on the ability of sensory neurons to extend neurites in response to neurotrophic factors as well as to regenerate after a preconditioning injury.

DISCUSSION

The accumulation of proteins damaged by formation of AGE residues in the peripheral nerve in diabetes has been linked to changes in nerve structure and neuronal function and development of diabetic neuropathy (32). We have
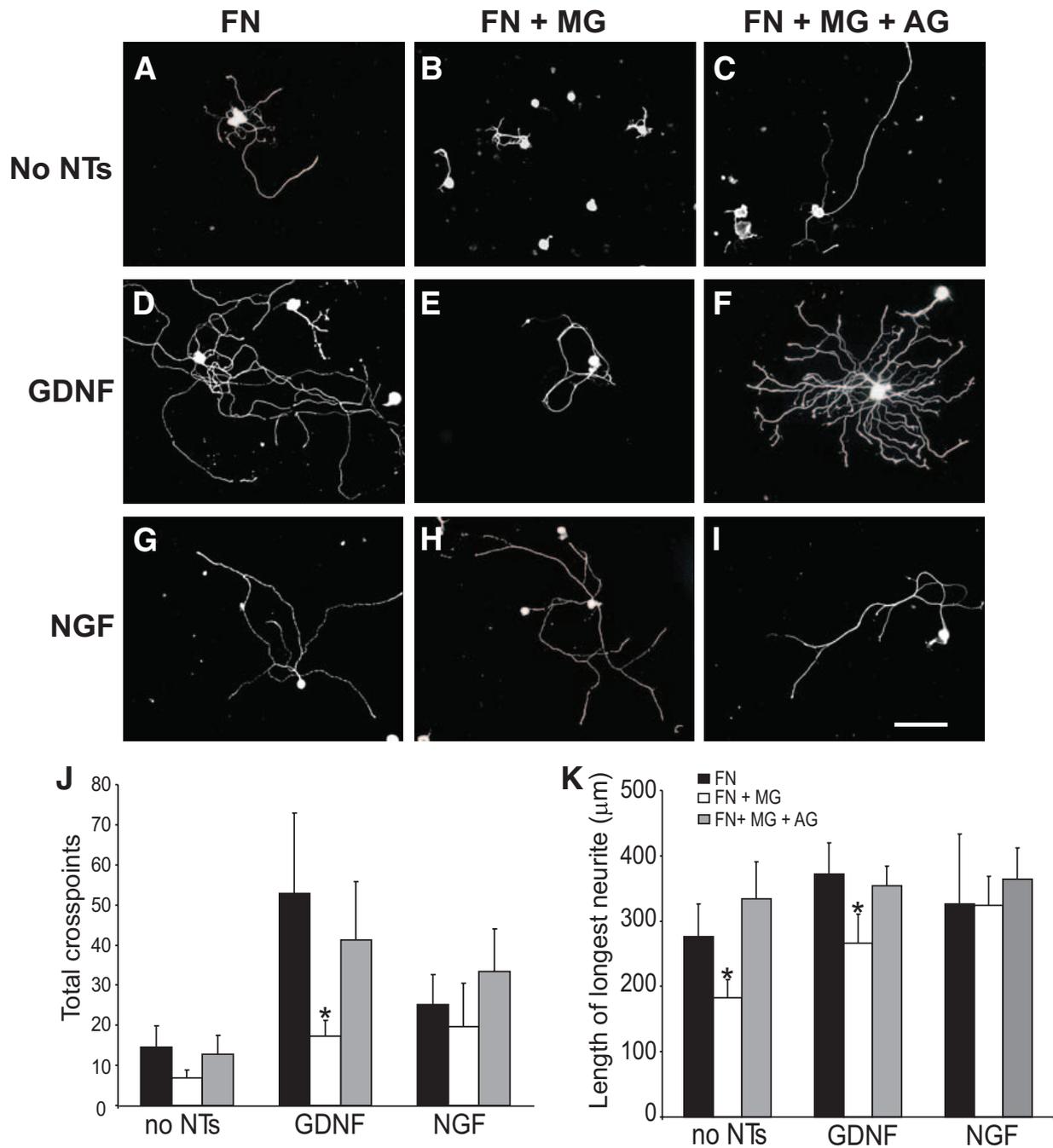
FIG. 5. Enhanced neurite outgrowth in response to a preconditioning sciatic nerve crush is reduced in neurons plated on glycated fibronectin. Representative photomicrographs of neurons from L4 and L5 DRG ipsilateral to a crush injury to the sciatic nerve (7 days before culture), which were dissociated and plated on fibronectin (*A*, *D*, and *G*), fibronectin glycated with methylglyoxal (*B*, *E*, and *H*), or fibronectin treated with methylglyoxal in the presence of aminoguanidine (*C*, *F*, and *I*) for 18 h with (*D–I*) or without (*A–C*) neurotrophin treatment (*D–F*, 50 ng/ml GDNF; *G–I*, 10 ng/ml NGF). The preconditioned neurons extend neurites in the absence of neurotrophic support (*A–C*); this was enhanced by neurotrophin treatment (*D–I*). Two parameters of neurite extension were quantified: total neurite outgrowth (*J*, cross points) and length of longest neurite (*K*). Neurons plated on glycated fibronectin showed a significant reduction in length of longest neurite and total neurite density compared with control, which was prevented by inclusion of the glycation scavenger aminoguanidine (*C*, *F*, and *I–K*) and also by NGF (*H*, *J*, and *K*). All data are expressed as means ± SD, $n = 4$ independent experiments (ANOVA with Bonferroni post hoc test, *$P < 0.05$). Scale bar = 100 µm. AG, aminoguanidine; FN, fibronectin; MG, methylglyoxal.

now conducted experiments that suggest that the glycation of two central ECM proteins associated with neuronal regeneration, laminin and fibronectin, may be linked directly to the failure of axonal regeneration in diabetic neuropathy. We have previously shown that cytosolic protein extracts of peripheral nerve of STZ-induced diabetic rats have increased fructosyl-lysine and AGE residue content (7). Here, we extend those findings by demonstrat-ing that ECM proteins are also glycated in the endoneurium of rat sciatic nerves. Moreover, glycation of ECM proteins with methylglyoxal increases AGE formation and decreases the ability of adult rat sensory neurons to extend neurites.

Endoneurial ECM proteins are glycated in vivo. The epidermis is innervated by the free axon terminals of small-diameter unmyelinated peptidergic and nonpeptidergic sen-

sory neurons (33). These subsets of sensory neurons differ in their responsiveness to specific neurotrophins. The peptidergic population expresses trkA and responds to NGF, whereas the nonpeptidergic population expresses receptors for GDNF: ret and GFR (34,35). Because it is the peripheral processes of these small-diameter neurons that degenerate in clinical (36) and experimental diabetic neuropathy (37–39), we focused our attention on the response of these populations of small-diameter neurons to ECM glycation.

Experimental diabetes in rats led to a profound increase in early glycation adduct and AGE residues in endoneurial ECM proteins of the sciatic nerve. The most abundant AGE residue was MG-H1, which increased $\sim$ fivefold after 6 weeks of diabetes. Similarly, fructosyl-lysine residue content increased from sixfold after 3 weeks of diabetes to 13-fold after 12 weeks. This is a higher increase than that seen for plasma glucose concentration but nevertheless is in keeping with the high (14-fold) increase of glucose concentration reported in sciatic nerve in STZ-induced diabetic rats (40). The fivefold increased content of MG-H1 residues is higher than the twofold increase in plasma concentration of methylglyoxal in STZ-induced diabetic rats and may reflect downregulation of glyoxalase 1, which provides the major defense against methylglyoxal glycation in diabetes (41,42). The accumulation of MG-H1 residues may be particularly damaging as it targets functional domains of ECM proteins, particularly arginine residues of RGD and GFOGER motifs, which are the major integrin-binding motifs (43,44).

Glycation of laminin and fibronectin in vitro. Further evidence for the reactivity of ECM proteins toward glycation was obtained by glycation of fibronectin and laminin in vitro. We used conditions for glycation by methylglyoxal where similar preparation of HSA produced a low or minimal extent of modification (2.49 equivalents of MG-H1 per mol [45]). Fibronectin and laminin were modified by methylglyoxal to produce 28 and 56 MG-H1 residues per mol protein, respectively. The arginine residue equivalents in these incubations of HSA, fibronectin, and laminin were 2.40 mmol/l, 1.86 mmol/l, and 2.50 mmol/l, and the concentrations of MG-H1 residues formed in methylglyoxal-modified HSA, fibronectin, and laminin were 2.5 mmol/l, 4.2 mmol/l, and 4.1 mmol/l, respectively. Assuming pseudo first-order reaction kinetics for the reaction of methylglyoxal with arginine residues in these proteins, fitting of these data to a first-order integrated rate equation indicates under the conditions studied the mean reactivity of arginine residues in fibronectin and laminin is circa three- to fourfold higher than in HSA. As the RGD residues are preferentially modified, it is likely that the reactivities of arginine residues in RGD motifs of laminin and fibronectin are much higher than this. These deductions provide support for proposing ECM proteins as targets for hot spot dicarbonyl glycation in diabetes.

Similar considerations for the formation of fructosyl-lysine residues in the glycation of HSA (22) fibronectin and laminin by glucose show that the final increased concentrations of fructosyl-lysine residues in the incubation were 114 μmol/l, 8 μmol/l, and 152 μmol/l. As neither lysine residues nor glucose were markedly depleted in these reactions, an appropriate kinetic comparison may be made by considering these data as a measure of initial rates of glycation. The lysine residue concentrations in the incubations of 6.6 mg/ml HSA, fibronectin, and laminin are circa 5.9 mmol/l, 1.2 mmol/l, and 2.3 mmol/l, respectively. The reactivity of lysine residues toward formation of fructosyl-lysine residues in HSA, fibronectin, and laminin is in the ratio 1:0.35:3.5 (not accounting for fructosyl-lysine residue degradation). Glycation of ECM proteins by methylglyoxal in vivo is likely to originate from methylglyoxal formed from cellular metabolism. High-dose thiamine therapy decreased plasma methylglyoxal concentration and glycation of aortal collagen by methylglyoxal by correction of dysfunctional cell metabolism downstream of glucose, without change in fructosyl-lysine residue content (46). Together, our data show that laminin is particularly susceptible to glycation by glucose.

ECM glycation dramatically impairs neuronal outgrowth and regeneration. Glycation of laminin with glycoraldehyde (47) or glucose (48) has previously been shown to reduce attachment and neuritogenesis in neonatal sensory neurons (47) and neurite extension from mouse DRG explants (48). In this study, we use two models of regeneration to demonstrate that methylglyoxal-glycation of laminin and fibronectin causes a reduction in neurite outgrowth from specific populations of sensory neurons after stimulation with neurotrophins and a reduction in preconditioned neurite outgrowth. Glycation of fibronectin with methylglyoxal impairs adhesion of smooth muscle cells (49), retinal pericytes (50), and endothelial progenitor cells (51). Similarly, methylglyoxal glycation of the RGD domain of collagen IV inhibits $\alpha v \beta_3$ integrin binding and endothelial cell adhesion (43,44). We previously implicated $\alpha 5 \beta 1$ integrin binding to the RGD domain of fibronectin as being of key importance in the neurite outgrowth of preconditioned neurons (23) and suggest that glycation of the RGD domain is also responsible for the impaired neurite outgrowth on glycated fibronectin. ECM integrin binding not only provides a physical anchor point between the intracellular actin cytoskeleton and the outside environment, enabling traction to mechanically drive axonal outgrowth, but also directly regulates important intracellular signaling cascades and subsequent gene transcription at the site of the focal adhesion (52). Indeed, using Affymetrix gene microarray analysis we have identified over 500 genes whose expression is significantly altered in NGF-treated neurons plated on methylglyoxal-glycated laminin compared with unmodified laminin (data not shown). Replacement therapy with exogenous NGF in diabetic rats normalizes key molecular and functional aspects of neuropathy in vivo (53,54). Although the mechanism of the observed NGF-induced rescue of axonal regeneration on glycated fibronectin remains to be elucidated, our initial experiments suggest it is not mediated via RAGE (receptor for AGEs) because function-blocking experiments using anti-RAGE did not affect neurite outgrowth on glycated fibronectin.

Failure of axonal regeneration is a key feature of both clinical and experimental diabetic neuropathy (55). In uninjured peripheral nerve samples from patients with diabetic neuropathy, clusters of regenerating axons can initially be observed alongside degenerating axons; however, as the disease progresses there is a decline in the number of regenerating axons (29). The regenerative response of the peripheral nerve after injury is also blunted in diabetes; little axonal regeneration is observed after sural nerve biopsy (56) or epidermal nerve fiber injury (57). We suggest that AGE accumulation in the endoneurial ECM may contribute to this progressive failure of axonal regeneration in diabetic neuropathy.

In conclusion, we have shown that ECM proteins are glycated in the endoneurium of rat sciatic nerves in

STZ-induced diabetes. Furthermore, glycation of laminin and fibronectin with methylglyoxal caused a reduction in both neurotrophin-stimulated and preconditioned neurite outgrowth from sensory neurons. This may provide a potential mechanism for the failure of collateral sprouting and axonal regeneration observed in diabetic neuropathy and may represent an important, if challenging, target for therapeutic intervention.

REFERENCES

1. Streuli CH. Integrins and cell-fate determination. J Cell Sci 2009;122:171–177
2. Letourneau PC, Shattuck TA. Distribution and possible interactions of actin-associated proteins and cell adhesion molecules of nerve growth cones. Development 1989;105:505–519
3. Tomaselli KJ, Doherty P, Emmett CJ, Damsky CH, Walsh FS, Reichardt LF. Expression of β1 integrins in sensory neurons of the dorsal root ganglion and their functions in neurite outgrowth on two laminin isoforms. J Neurosci 1993;13:4880–4888
4. Condic ML, Letourneau PC. Ligand-induced changes in integrin expression regulate neuronal adhesion and neurite outgrowth. Nature 1997;389:852–856
5. Vogelezang MG, Liu Z, Relvas JB, Raivich G, Scherer SS, Ffrench-Constant C. α4 integrin is expressed during peripheral nerve regeneration and enhances neurite outgrowth. J Neurosci 2001;21:6732–6744
6. Gardiner NJ, Fernyhough P, Tomlinson DR, Mayer U, von der MH, Streuli CH. α7 integrin mediates neurite outgrowth of distinct populations of adult sensory neurons. Mol Cell Neurosci 2005;28:229–240
7. Thornalley PJ, Battah S, Ahmed N, Karachalias N, Agalou S, Babaei-Jadidi R, Dawnay A. Quantitative screening of advanced glycation endproducts in cellular and extracellular proteins by tandem mass spectrometry. Biochem J 2003;375:581–592
8. Thornalley PJ. Glycation in diabetic neuropathy: characteristics, consequences, causes, and therapeutic options. Int Rev Neurobiol 2002;50:37–57
9. Brownlee M. Biochemistry and molecular cell biology of diabetic complications. Nature 2001;414:813–820
10. Thornalley PJ. Use of aminoguanidine (Pimagedine) to prevent the formation of advanced glycation endproducts. Arch Biochem Biophys 2003;419:31–40
11. Cameron NE, Cotter MA. Rapid reversal by aminoguanidine of the neurovascular effects of diabetes in rats: modulation by nitric oxide synthase inhibition. Metabolism 1996;45:1147–1152
12. Cameron NE, Gibson TM, Nangle MR, Cotter MA. Inhibitors of advanced glycation end product formation and neurovascular dysfunction in experimental diabetes. Ann N Y Acad Sci 2005;1043:784–792
13. Bradley JL, Thomas PK, King RHM, Watkins PJ. A comparison of perineurial and vascular basal laminal changes in diabetic neuropathy. Acta Neuropathol (Berl) 1994;88:426–432
14. Sharma AK, Thomas PK. Peripheral nerve structure and function in experimental diabetes. J Neurol Sci 1974;23:1–15
15. Powell H, Knox D, Lee S, Charters AC, Orloff MJ, Garrett RS, Lampert P. Alloxan diabetic neuropathy: electron microscopic studies. Neurology 1977;27:60–66
16. Yagihashi S. Nerve structural defects in diabetic neuropathy: do animals exhibit similar changes? Neurosci Res Commun 1997;21:25–32
17. Charonis AS, Tsilbary EC. Structural and functional changes of laminin and type IV collagen after nonenzymatic glycation. Diabetes 1992;41(Suppl.):49–51
18. McLellan AC, Thornalley PJ. Synthesis and chromatography of 1,2-diamino-4,5-dimethoxybenzene, 6,7-dimethoxy-2-methylquinoxaline and 6,7-dimethoxy-2,3-dimethylquinoxaline for use in a liquid chromatographic fluorimetric assay of methylglyoxal. Anal Chim Acta 1992;263:137–142
19. Karamoysoyli E, Burnand RC, Tomlinson DR, Gardiner NJ. Neuritin mediates nerve growth factor-induced axonal regeneration and is deficient in experimental diabetic neuropathy. Diabetes 2008;57:181–189
20. Ahmed N, Babaei-Jadidi R, Howell SK, Beisswenger PJ, Thornalley PJ. Degradation products of proteins damaged by glycation, oxidation and nitration in clinical type 1 diabetes. Diabetologia 2005;48:1590–1603
21. Simat TJ, Kleeberg KK, Muller B, Sierts A. Synthesis, formation, and occurrence of contaminants in biotechnologically manufactured L-tryptophan. Adv Exp Med Biol 1999;467:469–480
22. Ahmed N, Thornalley PJ. Chromatographic assay of glycation adducts in human serum albumin glycated in vitro by derivatization with 6-aminoquinolyl-N-hydroxysuccinimidyl-carbamate and intrinsic fluorescence. Biochem J 2002;364:15–24
23. Gardiner NJ, Moffatt S, Fernyhough P, Humphries MJ, Streuli CH, Tomlinson DR. Preconditioning injury-induced neurite outgrowth of adult rat sensory neurons on fibronectin is mediated by mobilisation of axonal α5 integrin. Mol Cell Neurosci 2007;35:249–260
24. Mostafavi-Pour Z, Askari JA, Whittard JD, Humphries MJ. Identification of a novel heparin-binding site in the alternatively spliced IIICS region of fibronectin: roles of integrins and proteoglycans in cell adhesion to fibronectin splice variants. Matrix Biol 2001;20:63–73
25. Westwood ME, Argirov OK, Abordo EA, Thornalley PJ. Methylglyoxal-modified arginine residues: a signal for receptor-mediated endocytosis and degradation of proteins by monocytic THP-1 cells. Biochim Biophys Acta 1997;1356:84–94
26. Agius E, Cochard P. Comparison of neurite outgrowth induced by intact and injured sciatic nerves: a confocal and functional analysis. J Neurosci 1998;18:328–338
27. Ide C. Peripheral nerve regeneration. Neurosci Res 1996;25:101–121
28. Smith DS, Skene JHP. A transcription-dependent switch controls competence of adult neurons for distinct modes of axon growth. J Neurosci 1997;17:646–658
29. Bradley JL, Thomas PK, King RHM, Muddle JR, Ward JD, Tesfaye S, Boulton AJM, Tsigos C, Young RJ. Myelinated nerve fibre regeneration in diabetic sensory polyneuropathy: correlation with type of diabetes. Acta Neuropathol (Berl) 1995;90:403–410
30. Hu-Tsai M, Winter J, Emson PC, Woolf CJ. Neurite outgrowth and GAP-43 mRNA expression in cultured adult rat dorsal root ganglion neurons: effects of NGF or prior peripheral axotomy. J Neurosci Res 1994;39:634–645
31. Edstrom A, Ekström PAR, Tonge D. Axonal outgrowth and neuronal apoptosis in cultured adult mouse dorsal root ganglion preparations: effects of neurotrophins, of inhibition of neurotrophin actions and of prior axotomy. Neurosci 1996;75:1165–1174
32. Thornalley PJ. Glycation in diabetic neuropathy. Characteristics, consequences, causes and therapeutic options. Intern Review of Neurobiology 2002;50:37–57
33. Hilliges M, Wang L, Johansson O. Ultrastructural evidence for nerve fibers within all vital layers of the human epidermis. J Invest Dermatol 1995;104:134–137
34. Wright DE, Snider WD. Neurotrophin receptor mRNA expression defines distinct populations of neurons in rat dorsal root ganglia. J Comp Neurol 1995;351:329–338
35. Bennett DL, Michael GJ, Ramachandran N, Munson JB, Averill S, Yan Q, McMahon SB, Priestley JV. A distinct subgroup of small DRG cells express GDNF receptor components and GDNF is protective for these neurons after nerve injury. J Neurosci 1998;18:3059–3072
36. Kennedy WR, Wendelschafer-Crabb G, Johnson T. Quantitation of epidermal nerves in diabetic neuropathy. Neurology 1996;47:1042–1048
37. Christianson JA, Riekhof JT, Wright DE. Restorative effects of neurotrophin treatment on diabetes-induced cutaneous axon loss in mice. Exp Neurol 2003;179:188–199
38. Beiswenger KK, Calcutt NA, Mizisin AP. Epidermal nerve fiber quantification in the assessment of diabetic neuropathy. Acta Histochem 2008
39. Toth C, Brussee V, Zochodne DW. Remote neurotrophic support of epidermal nerve fibres in experimental diabetes. Diabetologia 2006
40. Low PA, Yao JK, Kishi Y, Tritschler HJ, Schmelzer JD, Zollman PJ, Nickander KK. Peripheral nerve energy metabolism in experimental diabetic neuropathy. Neurosci Res Commun 1997;21:49–56
41. Thornalley PJ. Glyoxalase I: structure, function and a critical role in the enzymatic defense against glycation. Biochem Soc Trans 2003;31:1343–1348
42. Thornalley PJ. Dietary AGEs and ALEs and risk to human health by their interaction with the receptor for advanced glycation endproducts (RAGE): an introduction. Mol Nutr Food Res 2007;51:1107–1110
43. Pedchenko VK, Chetyrkin SV, Chuang P, Ham AJ, Saleem MA, Mathieson PW, Hudson BG, Voziyan PA. Mechanism of perturbation of integrin-mediated cell-matrix interactions by reactive carbonyl compounds and its implication for pathogenesis of diabetic nephropathy. Diabetes 2005;54:2952–2960

44. Dobler D, Ahmed N, Song L, Eboigbodin KE, Thornalley PJ. Increased dicarbonyl metabolism in endothelial cells in hyperglycemia induces anoikis and impairs angiogenesis by RGD and GFOGER motif modification. Diabetes 2006;55:1961–1969

45. Ahmed N, Thornalley PJ. Quantitative screening of protein biomarkers of early glycation, advanced glycation, oxidation and nitrosation in cellular and extracellular proteins by tandem mass spectrometry multiple reaction monitoring. Biochem Soc Trans 2003;31:1417–1422

46. Babaei-Jadidi R, Karachalias N, Ahmed N, Battah S, Thornalley PJ. Prevention of incipient diabetic nephropathy by high-dose thiamine and benfotiamine. Diabetes 2003;52:2110–2120

47. Luo ZJ, King RH, Lewin J, Thomas PK. Effects of nonenzymatic glycosylation of extracellular matrix components on cell survival and sensory neurite extension in cell culture. J Neurol 2002;249:424–431

48. Ozturk G, Sekeroglu MR, Erdogan E, Ozturk M. The effect of non-enzymatic glycation of extracellular matrix proteins on axonal regeneration in vitro. Acta Neuropathol (Berl) 2006;112:627–632

49. Sakata N, Meng J, Takebayashi S. Effects of advanced glycation end products on the proliferation and fibronectin production of smooth muscle cells. J Atheroscler Thromb 2000;7:169–176

50. Liu B, Bhat M, Padival AK, Smith DG, Nagaraj RH. Effect of dicarbonyl modification of fibronectin on retinal capillary pericytes. Invest Ophthalmol Vis Sci 2004;45:1983–1995

51. Bhatwadekar AD, Glenn JV, Li G, Curtis TM, Gardiner TA, Stitt AW. Advanced glycation of fibronectin impairs vascular repair by endothelial progenitor cells: implications for vasodegeneration in diabetic retinopathy. Invest Ophthalmol Vis Sci 2008;49:1232–1241

52. Streuli CH, Akhtar N. Signal co-operation between integrins and other receptor systems. Biochem J 2009;418:491–506

53. Apfel SC, Arezzo JC, Brownlee M, Federoff H, Kessler JA. Nerve growth factor administration protects against experimental diabetic sensory neuropathy. Brain Res 1994;634:7–12

54. Fernyhough P, Diemel LT, Hardy J, Brewster WJ, Mohiuddin L, Tomlinson DR. Human recombinant nerve growth factor replaces deficient neurotrophic support in the diabetic rat. Eur J Neurosci 1995;7:1107–1110

55. Thomas PK, Tomlinson DR. Diabetic and hypoglycaemic neuropathy. In *Peripheral Neuropathy*, 3rd ed. Dyck PJ, Thomas PK, Griffin JW, Low PA, Poduslo JF, Eds. Philadelphia, W.B. Saunders, 1992, p. 1219–1250

56. Sima AA, Bril V, Nathaniel V, McEwen TA, Brown MB, Lattimer SA, Greene DA. Regeneration and repair of myelinated fibers in sural-nerve biopsy specimens from patients with diabetic neuropathy treated with sorbinil. N Engl J Med 1988;319:548–555

57. Polydefkis M, Hauer P, Sheth S, Sirdofsky M, Griffin JW, McArthur JC. The time course of epidermal nerve fibre regeneration: studies in normal controls and in people with diabetes, with and without neuropathy. Brain 2004;127:1606–1615